2006

Numerical Analysis for Mixed Lubrication in Journal Bearings of Rotary Compressors

Takuya Hirayama
Toshiba Corporation

Kazuhiko Miura
Toshiba Corporation

Hitoshi Hattori
Toshiba Corporation

Yasutaka Ito
Toshiba Corporation

Numerical Analysis for Mixed Lubrication in Journal Bearings of Rotary Compressors

*Takuya Hirayama[1], Kazuhiko Miura[1], Hitoshi Hattori[2], Yasutaka Ito[2]

[1] Toshiba Carrier Corporation, Compressor Engineering Department
336, Tadewara, Fuji-shi, Shizuoka-ken, 416-8521, JAPAN
Tel: +81-545-62-5642, Fax: +81-545-66-0305
E-mail: takuya1.hirayama@toshiba.co.jp

[2] Corporate Research & Development Center, Toshiba Corporation
1, Komukai-toshiba-cho, Saiwai-ku, Kawasaki-shi, 212-8582, JAPAN
Tel: +81-44-549-2380, Fax: +81-44-549-2380
E-mail: hit.hattori@toshiba.co.jp

ABSTRACT

We have developed an analytical method for mixed lubrication in order to predict presence/absence, location, and magnitude of solid contact under any operational conditions of a rotary compressor bearing. This analytical method provides a solution by coupling a modified Reynolds equation and an elastic contact equation in consideration of surface roughness, also considering elastic deformation of a surface of a bearing.

In this paper, we present an example of an application of the analysis providing our finding in that an effect of surface roughness on a lubrication characteristic of the bearing has been known. In addition, we present an effect of improving the lubrication characteristic, when a surrounding groove is made on the bearing to deform easily the bearing surface. Furthermore, we mention a degree of occurrence of solid contact, when lubrication oil viscosity is reduced.

1. INTRODUCTION

A rotary compressor used for a recent heat-pump system is operated under higher pressure because of use of an environment-friendly refrigerant, such as R410A and CO_2. Additionally, its operating speed varies more widely by an inverter control to save energy. As a result, a lubrication condition of the bearing becomes severe. In particular, in a low speed region where an ability of forming a fluid lubrication film is low, a local mixed lubrication occurs frequently. The mixed lubrication condition causes increase in friction loss of the bearing. In the worst case, a compressor breaks down because of wear-out or seizing-up of the bearing. Therefore, in order to keep reliability and high performance, it is need to predict the characteristics of such a mixed lubrication accurately in the design phase by numerical analysis.

From the background stated above, we have developed a method for analyzing mixed lubrication of the rotary compressor bearing. We describe below an outline of this analytical method and findings obtained from the results of the analysis.

2. LUBRICATION CONDITION OF ROTARY COMPRESSOR BEARING

Fig. 1 shows the mechanism of a rotary compressor for applying the present analysis. This compressor has two compression chambers, and compression is operated alternately with a phase difference of 180 degrees [1,2]. The crankshaft which drives rolling pistons is supported by journal bearings positioned over and under the compression chambers. The crankshaft is acted with gas loads and imbalanced loads to cause bending deformation and, thus, has a tendency to tilt in the bearing resulting in thinning a lubrication oil film in an end of the bearing. As a countermeasure, as shown in Fig.2, a surrounding groove is made on the bearing in order to acquire easy elastic deformation of a bearing surface against a tilted crankshaft.

If the lubrication oil film is thinned, as shown in Fig. 3, solid contact may appear in fluid lubrication film. This status is called mixed lubrication. According to an increase in a proportion of solid contact, friction loss of the bearing increases. When a further increase in the proportion of solid contact exceeds a limit, surface injury occurs to result in breakdown of the compressor. Consequently, if presence/absence, location, and magnitude of solid contact can be known, the compressor can be prevented a failure, and has high performance operation maintained.

3. ANALYSIS FOR MIXED LUBRICATION

3.1 Governing equations

The bearing load W can be divided between the oil film load and the solid contact load. Therefore, W is equal to the value obtained by integrating the oil film pressure p and the solid contact pressure p_c.

$$W - \iint p ds - \iint p_C ds = 0 \qquad (1)$$

Where, W: bearing load, p: oil film pressure, p_c: solid contact pressure, s: bearing area. The second term of the left side is reaction force R_A by the lubrication oil film and the third term is reaction force R_B of the solid contact part.
Oil film pressure p is calculated from a Patir-Cheng's modified Reynolds equation [3,4] in consideration of the effect of surface roughness.

$$\frac{\partial}{{R_J}^2 \partial\theta}\left(\Phi_\theta \frac{\bar{h}^3}{\mu}\frac{\partial p}{\partial\theta}\right) + \frac{\partial}{\partial z}\left(\Phi_z \frac{\bar{h}^3}{\mu}\frac{\partial p}{\partial z}\right) = 6\frac{U}{R_J}\frac{\partial h_T}{\partial\theta} + 12\frac{\partial h_T}{\partial t} \qquad (2)$$

Where, Φ_θ and Φ_z : correction factor of a pressurized flow in θ and z directions, $\bar{h}$: mean oil film thickness, h_T : local oil film thickness, μ : viscosity coefficient of the lubricating oil, R_J and U : a radius of crankshaft and a peripheral velocity, respectively. Here, local film thickness h_T is calculated by introducing equation (3) and error function theory.

In addition, in a bearing of a compressor, elastic deformation of the bearing surface is considered. If it is assumed that deformation amount is δ and radial clearance between the bearing and the crankshaft is c, mean film thickness $\bar{h}$ is expressed by the following equation.

$$\bar{h} = c - x\cos\theta - y\sin\theta + \delta \qquad (3)$$

An amount of elastic deformation δ is, as shown in the following section, calculated by finite-element method after dividing a whole of the bearing by using a three-dimensional solid element. On the other hand, solid contact pressure p_C is calculated by applying an approximate expression[5] based on Greenwood and Tripp's elastic contact theory [6] for a surface roughness projection.

$$p_c = 4.4086\times10^{-5} k_c E' \left(4 - \frac{\bar{h}}{\sigma}\right)^{6.804} \qquad (4)$$

Where, k_C: a surface roughness constant according to a shape, E': a composite Young's modulus of the crankshaft and the bearing, σ : root- mean-square value of roughness of two surfaces.

Finally, numerical solution is deduced by applying the above-mentioned governing equations to make a balance in equation (1).

3.2 Analytical model of compressor bearing

A bearing (hereafter lower bearing) mounted on a lower position of the rotary compressor is analyzed in the present paper. Table 1 shows a pressure condition, a size, lubrication oil viscosity and physical property values, respectively. Moreover, effect of surface roughness was examined by analyzing surface roughness of the bearing and crankshaft by 2 species, i.e., R_{rms}=0.21 μm and 0.084 μm. R_{rms}=0.21 μm is a real measurement value before the operation and R_{rms}=0.084 μm is a real measurement value after the running-in operation for comparison to know the effect of improving the lubrication characteristic by the running-in operation. Fig.4 shows the finite element models[7] of the bearing with the surrounding groove (a) and without the surrounding groove (b) used in this analysis. Under such the condition, the mixed lubrication analysis was carried out by using a rotation frequency as a parameter and by changing from 9 to 90Hz.

4. RESULTS AND DISCUSSION

4.1 Effect of surface roughness

For the lower bearing, which has the surrounding groove, two surface roughness statuses of an initial operational period and a period after the running-in operation were analyzed. Fig. 5 shows the change of an oil film load and a solid contact load at 15-Hz rotation frequency during one cycle. (a) and (b) represent the initial operational period and the period after the running-in operation, respectively. Figs. 6 and 7 show the oil film pressure distribution and the solid contact surface pressure distribution at a 252-degree crank angle.

As known from Fig. 5, distinct solid contact takes place in the initial operational period in crank angles ranging from 210 to 330-degree and a solid contact load reaches 200N in a maximum. In contrast, it can be known that solid contact disappears after the running-in operation maintaining nearly a hydrodynamic lubrication condition. Reduced surface roughness improved an ability of fluid lubrication film formation, and reduced contact between projections.

Subsequently, as known from Figs. 6 and 7, in the initial operational period, the contact surface pressure distributes in a wide range and a peak of the contact surface pressure is higher than that of an oil film pressure. The solid contact force near the end part was generated by reduced thickness of the oil film around the end part by tilt of the crankshaft. On the other hand, after the running-in operation, the oil film pressure increases resulting in almost perfect disappearance of solid contact to cause reduction of a risk of wear-out and seizing-up.

Fig. 8 shows the analysis results of the solid contact force in two surface roughness statuses by using the rotation frequency as the parameter. From this figure, it can be known that the hydrodynamic lubrication condition can be maintained up to a low speed region by the running-in operation. In other words, it can be also known that using at a severe condition starting from the running-in operation requires surface processing of the crankshaft or the bearing to be able to improve initial affinity.

4.2 Effect of the surrounding groove

Description given below is of the result of examination of the presence/absence of the surrounding groove at the lower bearing end. The surface roughness status was calculated for values after the running-in operation. Figs. 9 and 10 each show the oil film pressure distribution and the solid contact surface pressure distribution in the 252-degree crank angle at 15-Hz rotation frequency.

As known from Fig. 9, in the bearing without the surrounding groove, solid contact occurred in the end part in the side of a compression chamber. The peak of the contact surface pressure is 30 times or more as high as that of the oil film pressure. In contrast, in the bearing with the surrounding groove, as known from Fig. 10, the oil film pressure becomes high and almost no solid contact can be observed. This is because the surrounding groove causes elastic deformation around the end part and because the clearance widens to leave from the crankshaft. The same factor causes for that solid contact occurs not in the end part but in the part near a bottom of the surrounding groove made in a small distance from the end part.

Fig. 11 shows the result of the analysis of the solid contact force for cases of presence/absence of the surrounding groove by using the rotation frequency as the parameter. It can be known that making the surrounding groove prevents occurrence of solid contact in a low speed range. As mentioned above, applying the present analytical method allows predicting the operational range which provides the effect of the surrounding groove.

4.3 Effect of lubrication oil viscosity

In this section, the results are presented for analysis of an effect of lubrication oil viscosity in the lower bearing with the surrounding groove. The surface roughness status is calculated by using values obtained after the running-in operation. Fig. 12 displays a relation between the lubrication oil viscosity and the solid contact force in 15-Hz and 30-Hz rotation frequencies. As known from this figure, the solid contact occurs in low viscosity region, and a further decrease of the viscosity increases the solid contact force. As stated above, a risky operation region can be decided by this analysis, when the lubrication oil viscosity is reduced due to the oil temperature rising and the refrigerant mixing.

5. CONCLUSIONS

In a rotary compressor bearing, elastic deformation of a bearing surface is considered, an analytical method for mixed lubrication has been developed to allow understanding solid contact, and the following findings were obtained by this analytical method.

1. When the surface roughness of the bearing is optimally smoothed in the running-in operation, an ability of fluid lubrication film formation is improved, and hydrodynamic lubrication range is widened on the bearing surface.
2. When a surrounding groove is made on the bearing, elastic deformation takes place around an end part, where solid contact occurs easily, to realize remarkable reduction of a peak of the contact surface pressure and enlargement of the hydrodynamic lubrication range.
3. A solid contact between the crankshaft and the bearing occurs in low viscosity region. The critical viscosity for keeping the hydrodynamic lubrication without solid contact can be found by this analysis.

We are using the present analytical method for the optimization of the bearing design and determination of allowable operating conditions of new development models. In the future, we continue to develop compressors having high reliability and high performance by using the present analytical method.

REFERENCES

1. Okoma, K., Tahata, M. and Tsuchiyama, H., 1990, Study of Twin Rotary Compressor for Air-conditioner with Inverter System, *Proceedings of The 1990 International Compressor Conference- at Purdue*, Vol.2, p.541-547.
2. Hattori, H and Kawashima, N., 1990, Dynamic Analysis of a Rotor-Journal Bearing System for Twin Rotary Compressors, *Proceedings of The 1990 International Compressor Conference- at Purdue*, Vol.2, p.750-760.
3. Patir, N., Cheng, H. S., 1978, An Average Flow Model for Determining Effects of Three Dimensional Roughness on Partial Hydrodynamic Lubrication, *Transaction of the ASME, Journal of Lubrication Technology*, Vol.100, No.1, p. 12-17.
4. Patir, N., et al., 1979, Application of Average Flow Model to Lubrication between Rough Sliding Surface, *Transaction of the ASME, Journal of Lubrication Technology.*, Vol.101, No.4, p. 220- 230.
5. Patir, N. and Cheng, H. S., 1978, Effect of Surface Roughness Orientation on The Central Film Thickness in E.H.D. Contacts, *Proceedings of The Institute of Mechanical Engineering Part 1*, Vol.185, No.48, p.15-21.
6. Greenwood, J. A. and Tripp, J. H., 1970, The Contact of Two Nominally Flat Surfaces, *Proceeding of the Institution of Mechanical Engineers.*, Vol.185, No.48, p. 625-633.
7. Hattori, H., 1998, EHL Analysis of A Journal Bearing for Rotary Compressors under Dynamic Loading (Effect of Flexible Structure at Bearing End), *Transactions of The Japan Society of Mechanical Engineers*, Part C, Vol.64, No.624, pp.3171-3178.

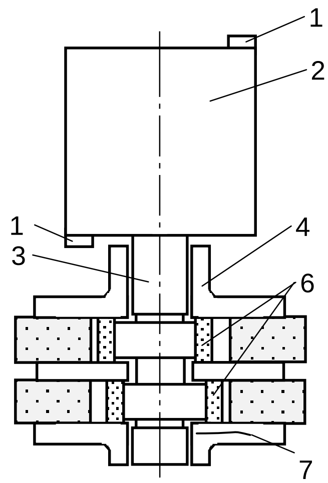

（a） mechanical section

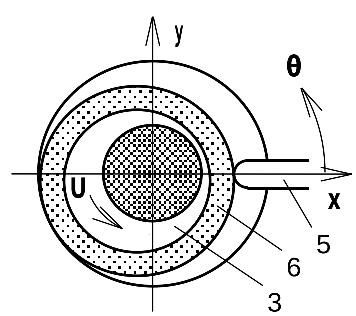

（b） Compression chamber

1. Balance weight 2. Motor rotor
3. Crankshaft 4. Upper bearing 5. Vane
6. Rolling piston 7. Lower bearing

Fig.1. Rotary compressor mechanism

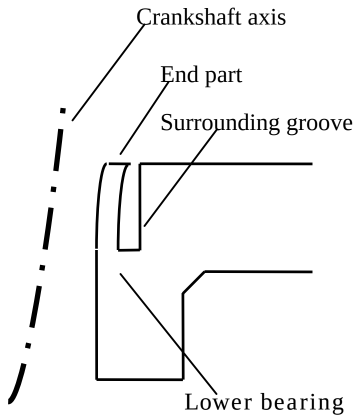

Fig.2. Flexible structure of lower bearing end

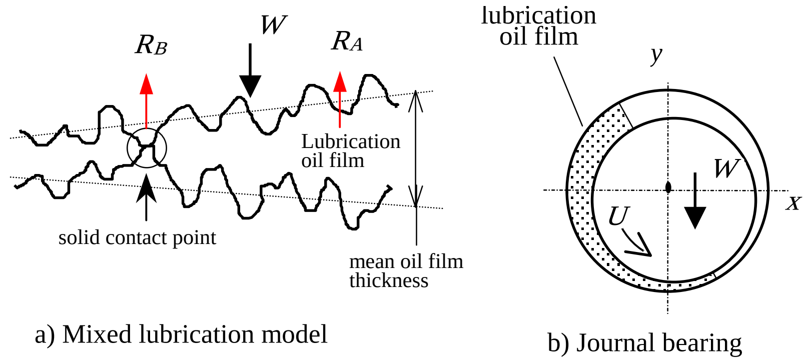

Fig.3. Mixed lubrication status of bearing surface

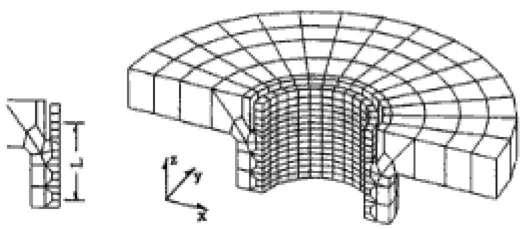

(a) With surrounding groove

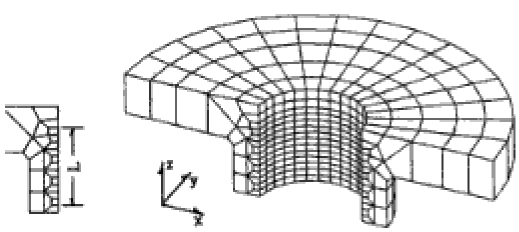

(b) Without surrounding groove

Fig.4. Finite element models of lower bearing

Table.1. Analysis conditions

Refrigerant		R410A
Discharge pressure	[MPa]	2.54
Suction pressure	[MPa]	0.087
Bearing diameter	[mm]	16.0
Radial clearance ratio		0.001
Oil viscosity	[Pa·s]	2.0×10^{-3}
Young's modulus	[N/mm2]	
(Crankshaft)		1.62×10^{5}
(Bearing)		1.18×10^{5}
(Composite)		1.50×10^{5}
Poisson's ratio		
(Crankshaft)		0.3
(Bearing)		0.3

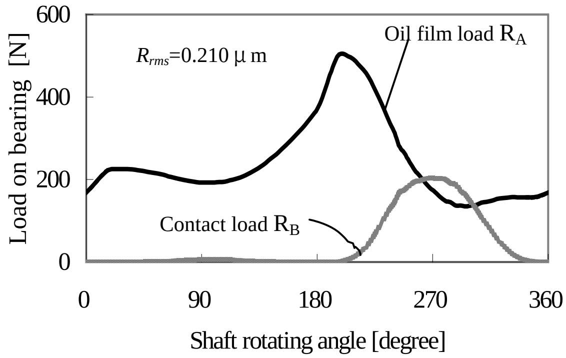

(a) Initial operation

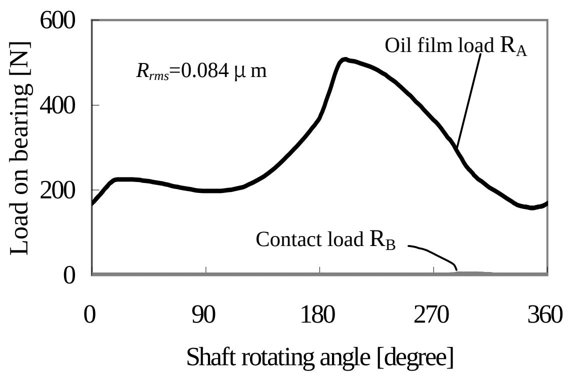

(b) After running-in

Fig.5. Variations of oil film load and contact load during 1 cycle

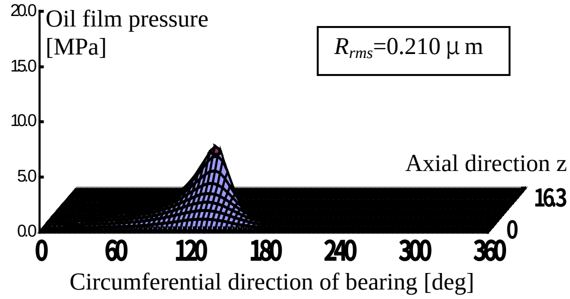

a) Oil film pressure distribution

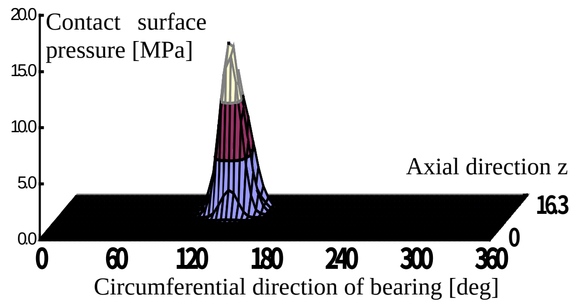

b) Contact surface pressure distribution

Fig.6. Pressure distributions on lower bearing in initial operation

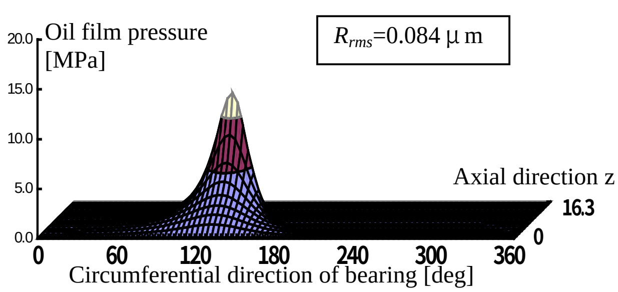

a) Oil film pressure distribution

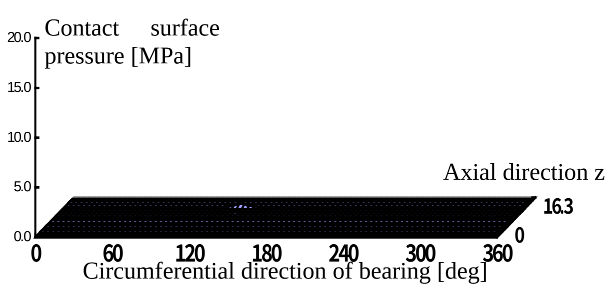

b) Contact surface pressure distribution

Fig.7. Pressure distributions on lower bearing after running-in

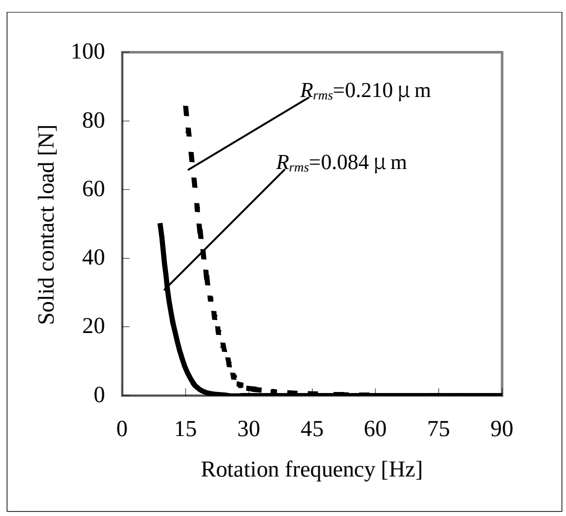

Fig.8. Improvement of bearing lubrication at low operating speed

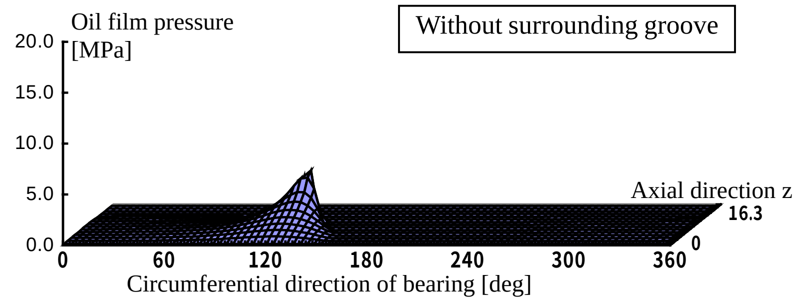

a) Oil film pressure distribution

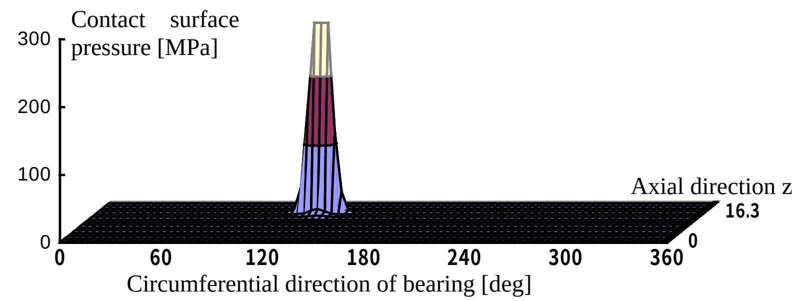

b) Contact surface pressure distribution

Fig.9. Pressure distributions on lower bearing without surrounding groove

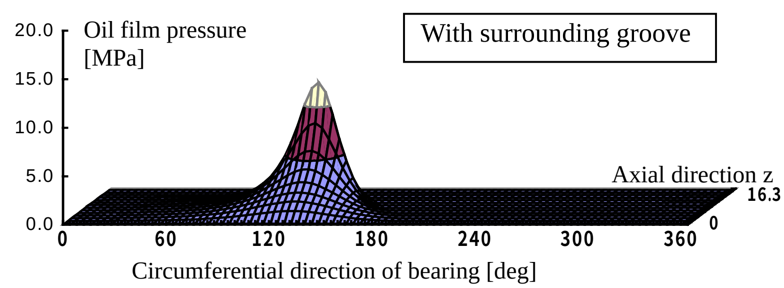

a) Oil film pressure distribution

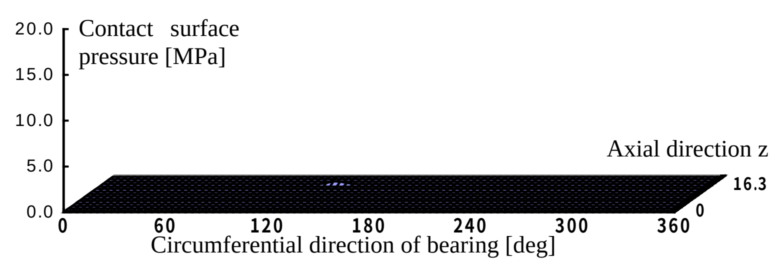

b) Contact surface pressure distribution

Fig.10. Pressure distributions on lower bearing with surrounding groove

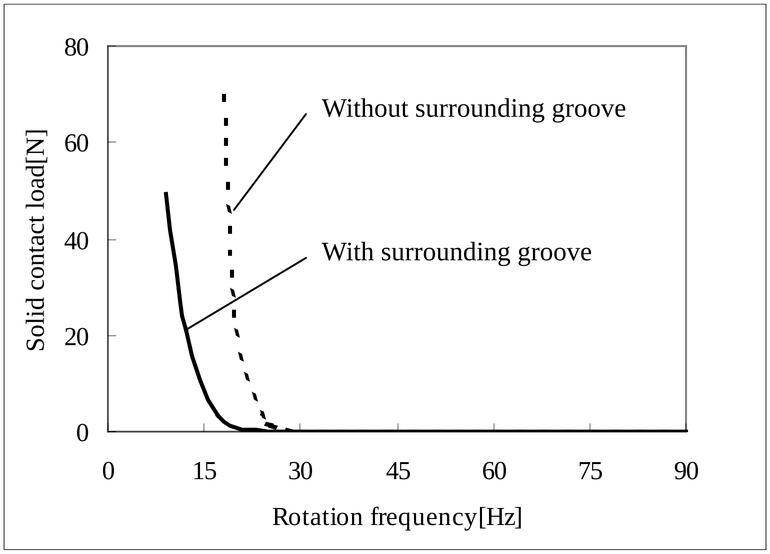

Fig.11. Improvement of bearing lubrication by making surrounding groove

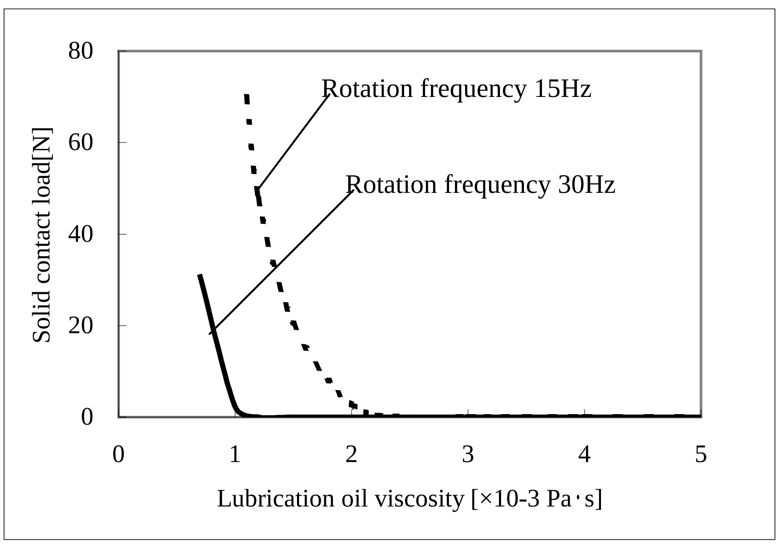

Fig.12. Relation between lubrication oil viscosity and solid contact load